

## Effects of J-Aggregation on the Redox Levels of a Cyanine Dye

J. R. Lenhard\* and B. R. Hein

*Imaging Research and Advanced Development, Eastman Kodak Company, Rochester, New York 14652-4708*

*Received: June 5, 1996; In Final Form: August 12, 1996*<sup>®</sup>

The effects of J-aggregation on the redox thermodynamics for a cationic cyanine spectral sensitizing dye are investigated. When adsorbed to the surfaces of cubic AgBr microcrystals, both the monomeric and J-aggregate forms of the cyanine dye can be reversibly oxidized with redox solutions containing ferricyanide or molybdicyanide complex. Diffuse reflectance spectra recorded for thin gelatin coatings of the dyed microcrystals after treatment with redox solution show distinct spectral bands associated with the dye and a stable, monooxidized dye radical ion. The fraction of dye oxidized can be accurately varied by simple adjustment of the electrochemical potential of the redox buffer solution. For the J-aggregated dye, the reflectance band for the dye shifts to shorter wavelengths and becomes significantly broadened with increasing fractional degree of oxidation. The formal oxidation potential for the adsorbed dye can be obtained from a Nernstian plot of redox-solution potential  $E$  vs  $\log [\text{oxidized dye}]/[\text{dye}]$  as constructed from the reflectance spectral data. The results indicate that the one-electron oxidation potential of the monomer on cubic AgBr to be lower than that of the J-aggregate by 74 mV. The energy of the singlet excited state of the J-aggregate is calculated to be lower than that of the monomer by a much larger amount. For the cationic dye in this study, the aggregation-induced changes in redox potential result in dramatic differences in the comparative photoresponses of the monomer and aggregate dye systems.

### Introduction

Cyanine dyes are a technologically important class of redox molecules that are commonly used as spectral sensitizers for photographic silver halide materials. Perhaps the most interesting property of these dyes is the ability to self-organize into one or more distinct aggregate configurations in solution and at liquid/solid and liquid/air interfaces.<sup>1</sup> As their optical spectroscopy indicates, the strong intermolecular interactions that exist between the tightly packed dye molecules within an aggregate can significantly affect dye energetics. Aggregation produces dramatic shifts in the absorption maximum and distinct alterations in absorption band shape relative to that observed for the monomeric dye. The J-aggregates are characterized by an intense narrow-band absorption that is red-shifted from the isolated monomer, whereas for H-aggregates the spectral absorption is hypsochromically shifted from the monomer band. Changes in dye excited-state lifetime and fluorescence yield also often accompany the formation of the H- or J-aggregate.<sup>2</sup> In addition, the efficiencies of processes such as energy transfer and electron transfer are known to be sensitive to the aggregation state of the dye.<sup>3</sup>

Much of our understanding of the relationship between cyanine dye energetics and the ability to photosensitize silver halide is based on electrochemical potential data. One-electron oxidation potentials have been shown to correlate with the HOMO level of the dye and thus provide a measure of the electron-donating and hole-trapping ability of the dye's ground state. The energy of the dye's excited state can be calculated using the oxidation potential and optical excitation data<sup>4</sup> or can be approximated using the one-electron reduction potential of the dye. Electrochemical potentials are typically measured for the monomeric dye dissolved in a nonaqueous solution.<sup>5</sup> In practice, however, most cyanines function as J-aggregate species when adsorbed to silver halide microcrystals. Despite the mechanistic insights about photosensitization that have been

gained using the available redox data,<sup>6</sup> no direct information exists on how aggregation phenomena influence the redox thermodynamics for cyanine dyes. Energy level estimates for dye aggregates adsorbed to silver halide crystals still rely on electrochemical data obtained for the unaggregated dye in solution.<sup>7</sup>

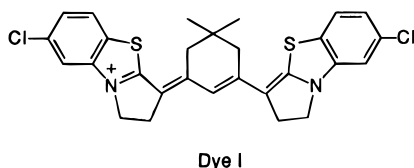
An estimate of the energetic consequences of aggregation can be obtained by comparing the optical transition energies for a specific dye chromophore in various states of association. The spectroscopic data reported for symmetrical thiacyanine dyes provide a point of reference for this estimate, as a predominance of the monomer, H-aggregate, and J-aggregate states can be achieved in aqueous solution by alterations in dye concentration and solution temperature.<sup>8</sup> The transition maxima for the dimer, trimer, tetramer, and other various blue-shifted H-aggregates and the red-shifted J-aggregate, span a range from about 480 to 625 nm. In terms of relative energy, these spectroscopic shifts correspond to perturbations in dye electronic-state energies as large as 0.6 eV. The extent to which these energy differences individually influence the ground and excited states is not presently known.

Unfortunately, the prospects for using standard electrochemical techniques to directly measure dye redox potential as a function of aggregation in solution are severely limited by the modest solubilities of cyanine dyes in aqueous electrolytes. The aggregation of cyanines in solution is extremely difficult to control, and because of their metastable character, mixtures of monomer dye and various polymeric aggregate species are often obtained. In the presence of a supporting electrolyte, the higher molecular weight aggregates readily precipitate. Solution electrochemical studies are further complicated by the fact that the self-association reactions for the dyes represent reversible equilibria.<sup>1,9</sup> Hence, dissociation of the solution aggregate can be expected to accompany changes in the oxidation state of an aggregate domain due to weakening of the lateral dye-dye interactive forces upon oxidation or reduction.

<sup>®</sup> Abstract published in *Advance ACS Abstracts*, October 1, 1996.

Adsorption of the cyanine molecules onto a solid surface, such as that on a silver halide crystal, offers greater control over the processes of aggregation. The aggregate state for many cyanines can often be manipulated through changes in dye structure, concentration, adsorption temperature, and by the utilization of molecular spacers. Strongly adsorbed dyes offer the added advantage that the aggregation processes can become largely irreversible. This feature, together with the fact that the substrate can lend additional structural stability to the aggregate, allows the redox chemistry of aggregated dyes to be examined without dissociative complications. Because the substrate can play a major role in defining the structure and properties of the aggregate, a method for measuring dye redox properties when adsorbed to silver halide is particularly desirable for probing silver halide photosensitizers.

In this paper we demonstrate that a cyanine dye adsorbed to silver halide microcrystals either as a monomer or as a well-defined J-aggregate can undergo reversible, one-electron oxidation reactions when treated with appropriate redox buffer solutions. The observed reversibility of the dye redox reactions permits the use of a potentiometric titration procedure to determine the formal redox potentials for cyanine dyes in the adsorbed state. A rigidized, red-sensitizing, thiadicarbocyanine dye I was chosen for this study because it exhibits an appropriate



oxidation potential, its stable oxidation product can be readily monitored spectroscopically, and its aggregation state on AgBr can be effectively controlled to be completely monomeric or predominantly J-aggregate by simple modification of the experimental conditions for dye adsorption.

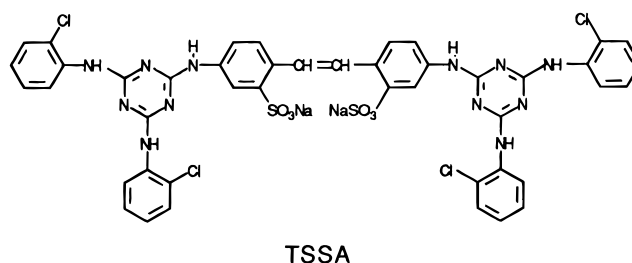
Included here is a study of the effects of molecule aggregation on the thermodynamics of dye sensitization of silver halide. The energies of the monomer and aggregate ground and excited states are obtained from the experimentally determined oxidation potentials and optical excitation energies. Energy diagrams indicate that J-aggregation results in a substantial lowering of the energy of the dye's excited state relative to the silver halide conduction band edge. Conclusions regarding the redox thermodynamics and mechanism of J-aggregate oxidation are supported by spectroscopic data obtained during the photoexposure of dyed AgBr microcrystals.

## Experimental Section

**Materials.** Reagent grade ascorbic acid, potassium ferrocyanide, potassium ferricyanide, ferric chloride hexahydrate, and phosphoric acid were obtained from Kodak Laboratory Chemicals and used without further purification. Potassium octacyanomolybdate(IV) was kindly synthesized by Dr. Jared Mooberry of Eastman Kodak Co. according to the procedure of Furman and Miller.<sup>10</sup> 3,8:3',12-dimethylene-9,11-neopentylthiadicarbocyanine *p*-toluenesulfonate (dye I) and 3,3'-disulfobutyl-5,5'-dichlorothiadicarbocyanine triethylammonium (dye II) were synthesized in the Dye Research Laboratory of Eastman Kodak Co. All redox solutions were prepared from water treated with a Milli-Q Water Purification System (Millipore).

**Preparation of AgBr Films.** The silver halide dispersion used consisted of 0.16  $\mu\text{m}$  edge-length cubic AgBr microcrystals that were internally doped with iridium hexachloroiridate ( $4 \times 10^{18}$  atoms/ $\text{cm}^3$ ) and precipitated by the double-jet precipitation

method in gelatin.<sup>11</sup> The dispersion had a pH of 5.6, pAg of 8.0, and a surface area of 1090  $\text{m}^2/\text{mol}$  Ag. The procedure for addition of sensitizing dye to the dispersion was dependent on the intended state of dye aggregation. To maximize the amount of dye adsorbed in the monomeric (unaggregated) state, the dispersion grains were pretreated with a triazinylstilbenesulfonic acid (TSSA) at a level ( $4.7 \times 10^{-4}$  mol of TSSA/mol of Ag)



that corresponds to ca. 80% of the saturation coverage for this AgBr dispersion. Dye was subsequently added to the treated dispersion at 40  $^{\circ}\text{C}$  from a methanol solution to give concentration levels ranging from  $2.0 \times 10^{-5}$  to  $2.0 \times 10^{-4}$  mol of dye/mol of Ag. The highest dye concentrations correspond to a maximum surface coverage of ca. 15% of full monolayer coverage. Preferential dye adsorption in the J-aggregated state was achieved by addition of dye to the dispersion, with no TSSA, at 70  $^{\circ}\text{C}$ . In some experiments methanol solutions of dye I and a companion, coaggregating dye were premixed in various proportions before addition to the dispersion at 70  $^{\circ}\text{C}$ .

The dye-sensitized dispersions were equilibrated for 20 min at the temperature of dye addition and subsequently diluted with additional gelatin solution. A gelatin hardening (cross-linking) agent was added, and the dispersion was then spread as a thin (ca. 5  $\mu\text{m}$  thick) film onto a transparent plastic support.

**Redox Potential Measurements.** Redox-mediator solutions were prepared in 0.02 M  $\text{H}_3\text{PO}_4$  (pH = 2.1) using various ratios  $\text{Fe}^{\text{II}}(\text{CN})_6^{4-}/\text{Fe}^{\text{III}}(\text{CN})_6^{3-}$  or  $\text{Mo}^{\text{IV}}(\text{CN})_8^{4-}/\text{Mo}^{\text{V}}(\text{CN})_8^{5-}$ . The phosphate buffer served to fix the pH and establish a specific ionic strength both in the redox solution and in the gelatin phase of the AgBr coating. Iron cyanide solutions of varying potential were made by mixing equimolar solutions of ferri- and ferrocyanide prepared from their respective potassium salts. Solutions of molybdicyanide were prepared by electrolysis of molybdocyanide at a 67  $\text{cm}^2$  area Pt gauze electrode by controlled potential coulometry using a Princeton Applied Research Corp. (PAR) Model 273 potentiostat in conjunction with a PAR 179 digital coulometer and a PAR 337A cell system. A constant total concentration of metal complex of 5 mM was maintained in all experiments. Potentiometric measurements of redox mediator solutions were made with the PAR Model 273 potentiostat and a glassy carbon disk electrode (Bioanalytical Systems, 1.6 mm diameter) that was polished with an aqueous slurry of 0.5  $\mu\text{m}$  alumina prior to use. Potentials were measured at  $22 \pm 1$   $^{\circ}\text{C}$  versus a KCl-saturated Ag/AgCl reference electrode. The reference electrode was calibrated before each experiment against a second Ag/AgCl reference electrode used as a laboratory standard. Diffuse reflectance spectra were obtained using a Varian 2400 UV-vis-near-IR spectrophotometer fitted with an integrating sphere (4.5 in. diameter, Halon coated). Film samples ( $3.5 \times 3.5$  cm, containing  $5 \times 10^{-8}$  mol dye) were immersed for 0.5 min in 800 mL of a stirred solution containing 5 mmol of the metal complex, blotted to detach adherent solution, and attached to the integrating sphere using a 0.25 in. thick disk of polished  $\text{BaSO}_4$ . Spectra were recorded from 950 to 450 nm at 5 nm/s versus an electronically stored spectrum of a coating of an undyed AgBr

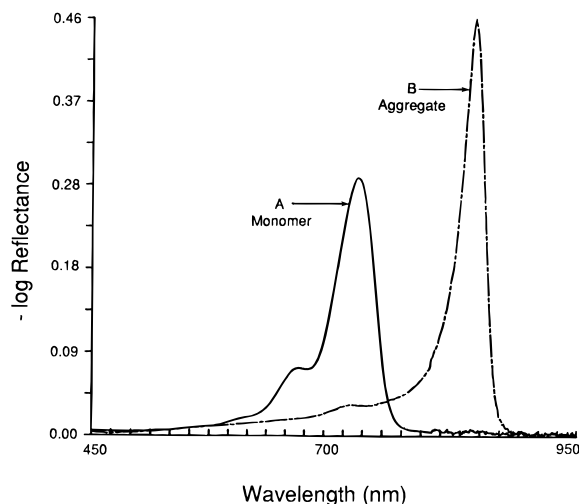


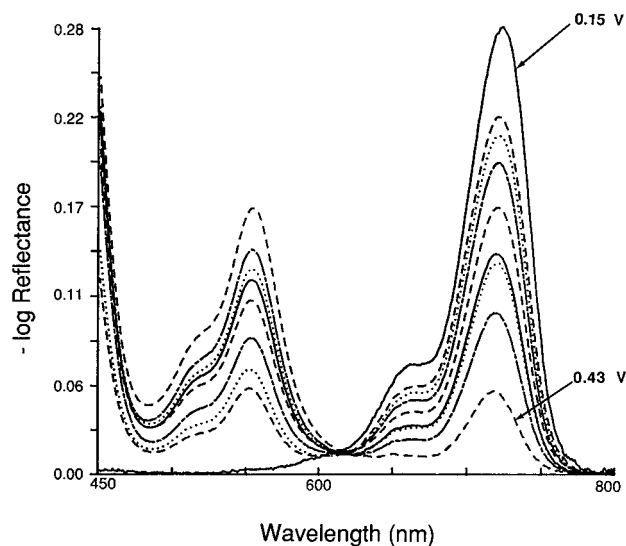
**Figure 1.** Reflectance spectra for coatings of dye I adsorbed to cubic AgBr microcrystals. Dye level is 0.2 mmol of dye I per mole of AgBr: (a) dye adsorbed as a monomer at 40 °C; (b) dye adsorbed as J-aggregate at 70 °C.

dispersion that was similarly treated with the redox solution. A separate AgBr film sample was used for each change in solution potential. In general, there was no change in reflectance spectrum of a coating after a duplicate spectral recording, indicating that any photoexposure incurred during routine measurement contributed little to the observed spectral changes. All experiments were performed under minimum safelight (Kodak 7B safelight filter) conditions.

**Photoexposures.** A 150 W xenon arc lamp (Osram) powered by an Oriol arc lamp supply Model 68742 was used as the continuous light source. The lamp output was passed through a monochromator (Oriol) for 435 nm exposures or through Kodak Wratten gelatin filter No. 2A and narrow-band interference filters (Oriol) to selectively expose at 725 or 850 nm. Coating samples were irradiated at room temperature at a distance of 20 cm from the lamp housing (Oriol) focusing lens where the incident light beam had a physical diameter of 5 cm. The lamp intensities were measured with an EG&G Model 450-1 radiometer with a Model 550-2 multiprobe detector. Timed exposures (0.5–15 s) were made with a Uniblitz shutter that was controlled using a PAR Model 173 universal programmer. Exposed samples were transferred within a few seconds to the Varian 2400 for spectrophotometric assay of dye photobleach.

## Results and Discussion

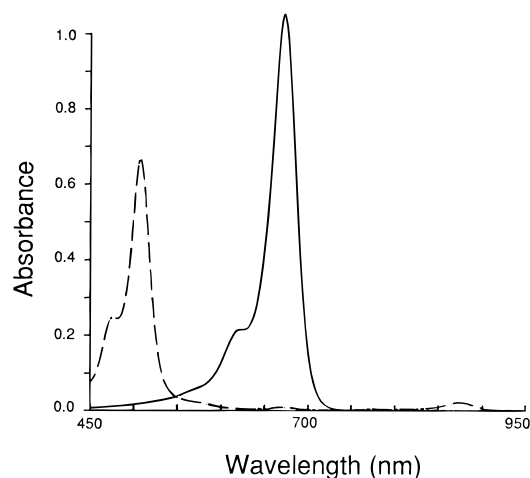
**Oxidation and  $E_M^{\circ}$  of Dye I Monomer.** Figure 1 shows diffuse-reflectance spectra recorded for the thin, gelatin coatings containing the dyed silver bromide microcrystals. These spectra demonstrate that the adsorption of dye I on cubic silver bromide can be constrained to be either monomeric or predominantly J-aggregate by modification of the conditions for dye adsorption. Pretreatment of the AgBr crystal surfaces with the stilbene deaggregating agent TSSA, followed by the addition of dye at a temperature of 40 °C, yields monomerically adsorbed dye. The anionic TSSA exhibits a modest affinity for AgBr and is thought to serve as a spacer to maintain separation between dye molecules.<sup>12</sup> The dye monomers are assumed to be isolated molecules adsorbed in a flat orientation with respect to the AgBr surface. Monomeric dye I (Figure 1A) exhibits a reflectance band at 722 nm on AgBr, which is shifted by 48 nm and slightly broadened (half-width,  $w^{1/2} = 948 \text{ cm}^{-1}$ ) relative to the absorption spectrum observed for the dye in methanol



**Figure 2.** Reflectance spectra for coatings of cubic AgBr microcrystals containing monomeric dye I after treatment with  $\text{Fe}(\text{CN})_6$  redox solutions ranging in potential from 0.15 to 0.43 V; pH = 2.1, 0.02 M  $\text{H}_3\text{PO}_4$ .

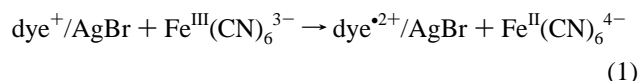
solution.<sup>13</sup> J-aggregate formation is favored by adsorption of the dye at 70 °C and in the absence of TSSA. Dye I J-aggregate (Figure 1B) exhibits a relatively narrow reflectance band ( $w^{1/2} = 523 \text{ cm}^{-1}$ ) with a maximum at 842 nm. The sharpness of the J-aggregate spectral band is consistent with a narrow distribution of aggregate sizes.<sup>2b,14</sup> J-aggregation also results in enhanced optical extinction; the molar extinction coefficient at  $\lambda_{\text{max}}$  for the aggregate is ca. 30% larger than that for the monomer dye. It is generally accepted that the J-aggregate is composed of planar, parallel dye molecules stacked plane-to-plane and end-to-end and are adsorbed to the AgBr surface along their long molecular edges with the short axis perpendicular to the surface. While J-aggregation at the AgBr/gelatin interface is common for dyes with shorter methine chain length, i.e., simple cyanine and carbocyanine dyes, the J-aggregate configuration is uncommon for dyes of the dicarbocyanine or tricarbocyanine class. Instead, these longer chain length dyes more typically adsorb as an H-aggregate.<sup>1</sup> This unusual aggregation characteristic for dye I is due to presence of the N–C and C–C hydrocarbon bridges, which provide for a rigid and largely planar molecular structure.

Figure 2 shows spectra recorded for a series of coatings containing monomeric dye I on AgBr that were equilibrated in various solutions of ferricyanide redox mediator for 0.5 min. The ferricyanide redox solutions were prepared in 20 mM  $\text{H}_3\text{PO}_4$  and ranged in potential from ca. 0.15 to 0.48 V vs Ag/AgCl. Increase in the oxidizing strength of the redox solution results in loss of the reflectance band associated with the dye monomer, at 722 nm, and concomitant growth of a new spectral band at 553 nm. The latter spectral band is due to the adsorbed, dye I radical dication and is bathochromically shifted 40–50 nm from the solution value. A vibronic shoulder is also evident at 514 nm. The solution absorption spectra recorded for dye I and its radical dication chemically generated in methanol are shown in Figure 3 for comparison purposes. In methanol the radical dication of dye I exhibits absorption bands at 507 nm,  $\epsilon_{\text{max}} = 18.3 \times 10^4 \text{ M}^{-1} \text{ cm}^{-1}$ , and 874 nm,  $\epsilon_{\text{max}} = 0.61 \times 10^4 \text{ M}^{-1} \text{ cm}^{-1}$ .<sup>15</sup> The similarities in the solution–surface spectral shifts observed for the dye and radical dication, together with the appearance of the isosbestic point at 612 nm, serve as evidence that both the dye and the oxidized form of dye I remain firmly adsorbed to the AgBr surface throughout the course of



**Figure 3.** Absorption spectra for a 5  $\mu$ M solution of dye I in methanol obtained before (—) and after (---) exhaustive one-electron oxidation with  $\text{FeCl}_3$ .

the experiment. The data of Figures 2 and 3 are consistent with the oxidation of dye I to the radical dication according to



The oxidation of adsorbed dye I monomer is fully reversible. Oxidation/reduction cycle experiments were conducted by treatment of a film sample with a ferricyanide solution of the highest oxidizing strength, followed by a chemical reduction with dilute ascorbic acid solution. A comparison of the reflectance spectra recorded before and after the oxidation/reduction cycle indicates the total loss of adsorbed dye I to be less than 3%. More importantly, no changes in spectral band shape or position resulted from this redox sequence. The AgBr adsorbed, dye I radical dication exhibits a half-life of ca. 30 min in these coatings that are saturated with aqueous ferricyanide solution.

Given the assumption that the equilibrium state of each AgBr/dye grain in the coating is determined by the electrochemical potential  $E_{\text{soln}}$  of the surrounding chemical redox solution, and by representing the surface activity with surface concentration  $\Gamma$ , the Nernst equation describing the dye oxidation process is written as

$$E_{\text{soln}} = E_{\text{M}}^{\circ'} + RT/nF \ln\{\Gamma_r/\Gamma_d\} \quad (2)$$

where  $\Gamma_d$  and  $\Gamma_r$  are the concentrations of adsorbed dye and radical dication, respectively, and  $E_{\text{M}}^{\circ'}$  is the formal oxidation potential for the adsorbed monomer.

Extraction of surface concentration data from the reflectance spectra of Figure 2 was made using linear calibration plots ( $[1/\text{reflectance}]$  vs  $\Gamma_d$ ) that relate dye concentration to the intensity of the dyes' reflectance band.  $\Gamma_r$  could be evaluated directly from the spectral band for the radical or by difference using  $\Gamma_d$  and the total surface concentration  $\Gamma_T$  of dye.<sup>16</sup>

Figure 4 shows a plot of the solution potential vs  $\log \Gamma_r/\Gamma_d$ . For values of  $\log \Gamma_r/\Gamma_d$  between  $-1$  and  $+1$ , which correspond to 10% and 90% oxidation, the experimental data can be approximately fit with a straight line. Averages from eight replicate experiments for dye I monomer (at the concentration level of  $0.2 \times 10^{-3}$  mol of dye/mol of Ag,  $2 \times 10^{-11}$  mol of dye/cm<sup>2</sup> of AgBr) indicate an intercept of  $0.355 \pm 0.008$  V and slope of  $102 \text{ mV} \pm 0.004 \text{ V}$ .

Although the data of Figures 2 and 4 suggest Nernstian behavior, the slope of the plot in Figure 4 differs markedly from

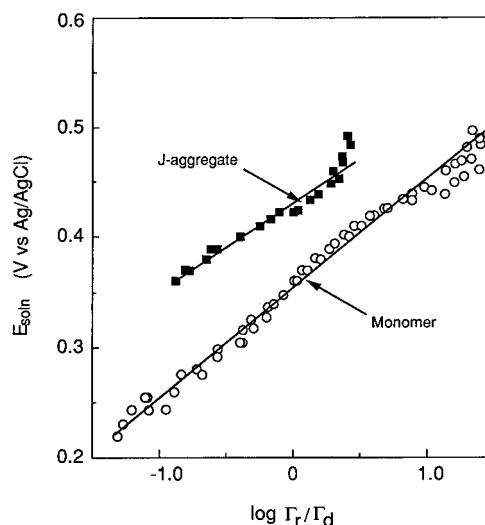


**Figure 4.** Nernst plot of redox solution potential vs  $\log [\text{oxidized dye}]/[\text{dye}]$  for dye I adsorbed in the monomeric and J-aggregate states.

the 59 mV/decade slope predicted by the classical Nernst equation for a one-electron transfer process. Similar nonideal behavior has been described for other redox molecules that are specifically adsorbed to electrode surfaces, contained in self-assembled monolayer structures, or incorporated into polymeric redox films. The nonidealities associated with these fixed-site redox reactions have been attributed to a variety of factors and include concentration-dependent surface activity coefficients,<sup>17</sup> inhomogeneity or a distribution of redox sites,<sup>18</sup> excess chemical potentials,<sup>19</sup> molecular dipole effects,<sup>20</sup> Donnan equilibria,<sup>21</sup> mechanical stress,<sup>22</sup> and surface electrostatic effects.<sup>23</sup> With the exception of inhomogeneity effects, most of these factors are thought to be relatively unimportant in the experiments described here and would not appreciably contribute to the observed non-Nernstian behavior. The electrochemical potential at the AgBr/dye/gelatin interface will, under ideal conditions, be dictated solely by the relative concentrations of ferri- and ferrocyanide in the mediator solution. It is possible, due to differences in gelatin diffusion coefficients or ion-pairing constants, that even under conditions of equilibrium, a disparity exists between the relative concentrations of the iron complex in the film with that in solution. The available evidence suggests, however, that the permeability of swollen gelatin polypeptide film toward water molecules, ferri/ferrocyanide ions, and the various counterions, is high and that access of the redox agent to the surface of the AgBr microcrystallites is not thought to be restricted by gelatin-polymer mechanics. The AgBr surface contains an excess of bromide ions, which stabilize the crystal and promote adsorption of the cationic sensitizing dye. In addition to halide ion, the dye microenvironment contains the TSSA anion, residual water, and gelatin molecules, each of which can interact chemically and electrostatically with the oxidized dye (and with the mobile ferricyanide ions) and hence may undergo redistribution at the crystal surface in an amount related to the fractional degree of dye oxidation. Reorganization within the crystal side of the interface, which would include movement of interstitial silver ions and modification of the space charge layer, may also occur in response to changes in surface charge density. Although surface electrostatic effects could be important, the effective dielectric constant of the gelatin layer, when saturated with the acidic phosphate electrolyte, is considered to be relatively large and thus should be able to compensate the excess surface charge created during dye oxidation.<sup>24</sup> Consistent with this notion, Nernst plots obtained for monomeric dye I were, within the experimental uncertainty,

found to be independent of mediator-solution electrolyte ( $\text{H}_2\text{PO}_4^-$ ) concentration from 0.02 to 0.1 M and invariant with dye concentration over the range of  $0.05 \times 10^{-3}$  to  $0.2 \times 10^{-3}$  mol of dye/mol of Ag.

A variety of evidence exists for heterogeneity in cyanine dye monolayers formed on silver halide and other solid surfaces. Dye adsorption,<sup>25</sup> fluorescence,<sup>26</sup> and photosensitization<sup>27</sup> data are particularly supportive of a distribution of dye states. Given this evidence for site heterogeneity, we favor a site distribution model to explain the nonideal Nernst slopes in Figure 4. In this model a distribution in ground-state levels, and hence in  $E^\circ$ , results from a range of specific AgBr site-dye interactions, Coulombic perturbations, and dye-dye orientation effects. Redox site heterogeneity has been previously represented by a Gaussian distribution of standard potentials about an average value as given by eq 3:

$$\frac{N_E}{N_T} = -\frac{1}{\sigma\sqrt{2\pi}} \exp\left\{-\frac{[E - E^\circ]^2}{2\sigma^2}\right\} \quad (3)$$

where  $N_E/N_T$  is the fraction of molecules with the formal potential  $E$ ,  $E^\circ$  is the formal potential at the center of the distribution, and  $\sigma$  is the spread (standard deviation) of formal potentials. As shown by Alberly et al.,<sup>18a</sup> a Gaussian distribution of redox potentials for adsorbed molecules will modify the slope of a Nernst plot according to

$$dE/d(\log \Gamma_r/\Gamma_d) = 0.059[\text{erf}(2RT/\sigma F)]^{-1} \quad (4)$$

Thus, a greater Nernst slope indicates a broader distribution of potentials. For the data of Figure 4, the 102 mV/decade slope corresponds to a Gaussian distribution of redox sites with a standard deviation of 64 mV. The full range of potentials encompassed by this distribution is  $\pm 3\sigma$  or ca. 400 mV. Because the intercepts for plots as represented in Figure 4 were found to be invariant with dye I surface concentration, we assign the intercept to the formal potential  $E_M^{\circ'}$  for the oxidation of dye I monomer on cubic AgBr.<sup>28</sup>  $E_M^{\circ'}$  represents the center of the dye redox distribution on the crystal surface.

To some extent, the redox potential of the adsorbed monomer may be influenced by the presence of the stilbenesulfonic acid deaggregating agent TSSA. TSSA can form association complexes with some cyanines in solution and can cause a red shift in the absorption maximum of the monomer of 2–15 nm. The spectrum of the adsorbed dye I monomer, however, is only very slightly (2–3 nm) shifted due to TSSA, indicating that the interaction energy between TSSA and dye I is rather small. This observation is consistent with TSSA acting simply as a spacer molecule and suggests that the extent to which TSSA itself modifies the dye oxidation potential is minimal.

It is also of interest to note that the value of  $E_M^{\circ'}$  is 145 mV less positive than the formal oxidation potential (0.500 V vs Ag/AgCl) measured for dye I in *acetonitrile* solution.<sup>29</sup> Part of this difference is related to the free energy change that is associated with the process of adsorbing the dye to the AgBr crystal. Other factors which also contribute to this difference between surface and solution potential include the dye cation/dication solvation energy differences between water and acetonitrile and the effects of reference electrode liquid junction potentials.<sup>30</sup>

**J-Aggregate Oxidation and  $E_{\text{Agg}}^{\circ'}$  Measurement.** Similar redox equilibration experiments conducted with gelatin film samples containing the J-aggregate of dye I adsorbed to the cubic AgBr grains yield reflectance spectral changes that are grossly different from those presented above for the dye monomer. The

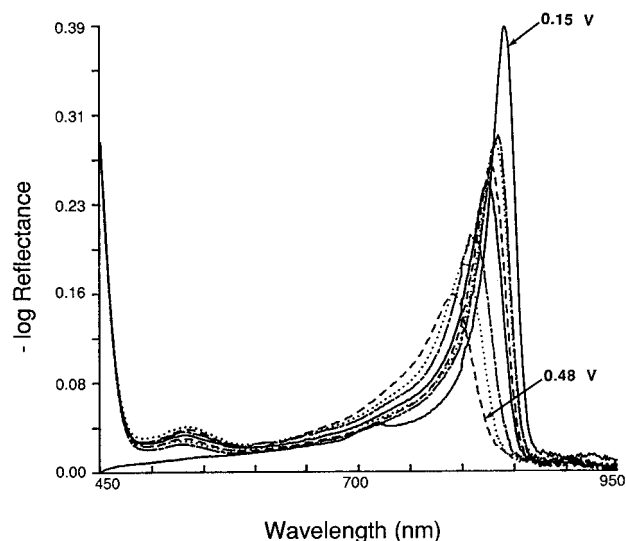


**Figure 5.** Reflectance spectra for coatings containing dye I J-aggregate recorded as a function of  $\text{Fe}(\text{CN})_6$  redox solution potential from 0.15 to 0.48 V.

series of spectra shown in Figure 5 demonstrate that the dye I J-aggregate can undergo electron exchange with solution  $\text{Fe}^{\text{III}}(\text{CN})_6$ , as the decrease in the intensity of the 842 nm band with increasing solution potential is consistent with J-aggregate oxidation. In contrast to the dye-monomer system, however, increase in fractional degree of dye oxidation is accompanied by a distinct broadening and shifting of the aggregate spectral band to shorter wavelengths. A striking aspect of these spectra is the relatively low intensity of the spectral band for the oxidized form of the aggregate at 533 nm, which appears in the same vicinity as the spectral band observed for the radical dication of the monomer. The latter finding suggests that the one-electron oxidation of the dye I J-aggregate is not a reversible process, but instead may result in aggregate destruction. This possibility is quite plausible given that the actual arrangement of the molecules within the dye aggregate results from a superposition of geometry-dependent attractive and repulsive forces. While dispersive van der Waals and dipole-dipole interaction terms comprise the attractive intermolecular forces, the repulsive forces are mainly electrostatic in nature. Oxidation of dye sites might be expected to dramatically increase the repulsive forces operative within the aggregate framework and as a consequence could possibly lead to aggregate dissociation.<sup>31</sup>

To examine this stability issue, oxidation/reduction cycle experiments like those described above for the monomeric dye were conducted on film samples containing aggregated dye I. For this analysis we utilized the more highly oxidizing  $\text{Mo}(\text{CN})_8^{3-}$  redox system so that the J-aggregate could be oxidized to a more appreciable extent.<sup>32</sup> Shown in Figure 6 are reflectance spectra recorded before and after oxidation with electrogenerated molybdicyanide and after subsequent reductive regeneration with ascorbic acid. Most interesting is the fact that curve C, which was obtained after the complete oxidation/reduction cycle, is a close replica of the spectrum of curve A, which was recorded before oxidation. This finding indicates that the J-aggregate, like the corresponding monomer, can be oxidized in a fully reversible manner as given by eq 1 and that the J-aggregate *does not dissociate upon oxidation*. In contrast, the J-aggregate physical structure remains intact in the oxidized state. The data of Figure 6 also show that, at this higher level of oxidation, the spectral band for the oxidized aggregate (at 533 nm) is more clearly defined and is very similar in position and shape to that observed for the monomer radical dication (at 553 nm). The apparent extinction coefficient for the oxidized

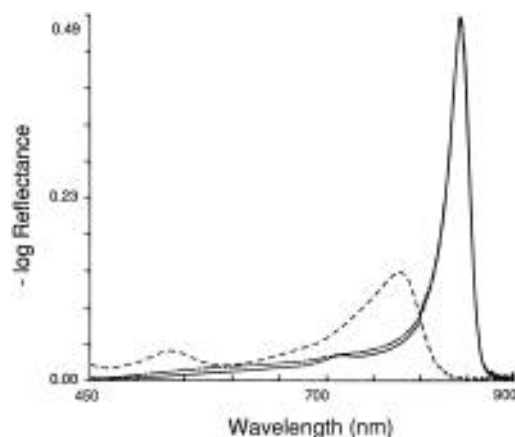
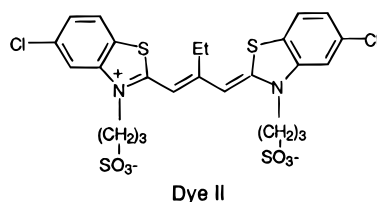


**Figure 6.** Reflectance spectra for coatings containing dye I J-aggregate recorded during a chemical oxidation/reduction cycle: (a) before (—) oxidation; (b) after (---) oxidation with a 0.68 V molybdocyanide solution; (c) after (— · —) subsequent reduction with a 0.1 V ascorbic acid solution.

J-aggregate molecule, however, for reasons that are unclear, is considerably lower in magnitude than that found for the oxidized dye I monomer.

The peculiar band broadening and wavelength shift that accompany the chemical oxidation of the J-aggregate provide some clues about the distribution of positive charge within these highly ordered systems. The spectral features shown in Figure 5 are very similar to those obtained in experiments where the average *physical* size of a J-aggregate is varied in a statistical sense by dilution with a second dye chromophore.<sup>33</sup> Control of the J-aggregate size for simple cyanine and carbocyanine dyes has been demonstrated using the dilution technique wherein the second dye is structurally similar to, but electronically distinct from, the primary dye. For *N,N'*-diethyl-2,2'-cyanine adsorbed to an octahedral AgBr substrate, variation in the mole fraction of the diluent dye from 0 to 0.94 was shown to cause a shift in the absorption maximum from 575 nm, that is characteristic of the pure J-aggregate, to a monomer-like 540 nm absorption. These spectral shifts are qualitatively consistent with a description of dye-dye interactions based on the point-dipole approximation.<sup>34</sup> Accompanying the dilution-induced spectral shift was a significant broadening of the J-aggregate absorption band.

We conducted related dye mixture experiments, where dye I and a companion dye were premixed in methanol and added to the silver bromide dispersion under conditions that favor J-aggregate formation. The anionic thiacyanine dye II was



found to be most compatible with dye I among a series of dyes examined for coaggregation purposes. The systematic dilution of the dye I J-aggregate is demonstrated in Figure 7, which shows reflectance spectra for a series of coatings that contain various proportions of dye I and anionic dye II. These spectra indicate that each chromophore retains an independent absorption band, yet the shape and peak position for each band systematically change with the dilution factor. A blue shift in the spectrum for dye I occurs with increasing dye II concentration. Although the spectra become slightly complicated at mole

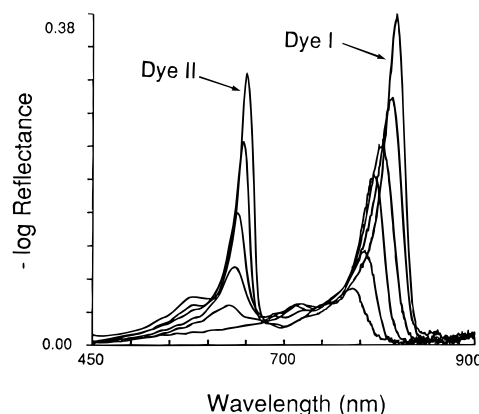


**Figure 7.** Reflectance spectra for coatings of cubic AgBr microcrystals containing mixtures of dye I and dye II. Mole fraction of dye I in mixture is 1.0, 0.90, 0.78, 0.56, 0.35, and 0.13.

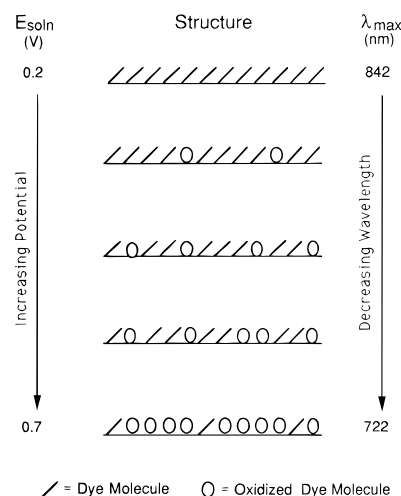


**Figure 8.** Model for dilution of J-aggregate during oxidation.

fractions less than 0.35 due to the presence of additional bands at 750 and 720 nm, the spectral changes that appear in Figure 7 closely mimic those that occur during the oxidation of the dye I J-aggregate as shown in Figure 5. Overall, the similarities in the spectral features that accompany J-aggregate oxidation and J-aggregate dilution support a model wherein the oxidized states behave as inert spacer units within the aggregate host structure. As schematically depicted in Figure 8, we propose that these oxidized sites are formed at locations that are spatially distributed across the aggregate domain, perhaps for purposes of minimizing repulsive electrostatic interactions between the dicationic molecules. As a result, the aggregate becomes segmented into populations of smaller effective size. As the physical size of the aggregate cluster is decreased, the effective size of the delocalized exciton is also decreased, and hence the observed shift in the transition energy.<sup>35</sup> Consistent with this view that the oxidized dye behaves as an isolated spacer in the J-aggregate framework is the appearance in the spectrum of the oxidized aggregate of an absorption band (at 533 nm), which closely resembles that of a *monomer* radical dication. The appearance of this monomer-like absorption argues against a band-type, electronic structure for J-aggregate "hole", i.e., oxidized, states. Clearly, hole mobility within the aggregate of dye I is far slower than the mobility of an exciton.

For a given value of the solution potential  $E_{\text{soln}}$ , the spectra of Figures 2 and 5 show that the degree of oxidation of the aggregate is less than that for the monomeric form of Dye I. Nernst plots constructed using the peak reflectance values for the J-aggregate also indicate the aggregate to be more difficult

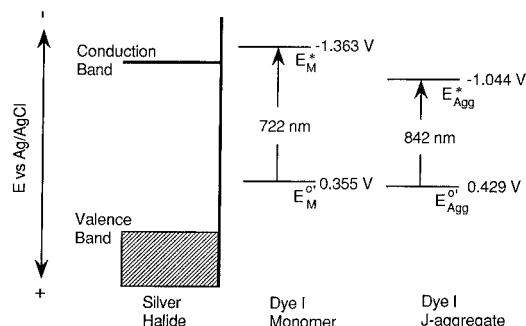


**Figure 9.** Energy level diagram for the spectral sensitization of silver bromide by dye I.

to oxidize than the monomer.<sup>36</sup> The one-electron oxidation potential for the aggregate  $E_{\text{Agg}}^{\text{o}'}$  as obtained from the intercept of the plot in Figure 4 is  $0.429 \pm 0.010$  V (five determinations).  $E_{\text{Agg}}^{\text{o}'}$  was independent of dye concentration from surface coverages of 0.05 to 0.2 mmol of dye/mol of Ag. Interestingly, the slope of the Nernst plot for the aggregate ( $92 \pm 19$  mV) is very similar to that obtained for the monomer, which suggests that the factors governing the deviation from an "ideal" Nernstian response are similar for these two distinct systems of adsorbed dye. Within the context of the  $E^{\text{o}'}$  distribution model, this result suggests that the spread in dye redox states is primarily the result of dye–substrate interactions.

#### Energy Level Considerations and Spectral Sensitization.

Using the oxidation potential data  $E_{\text{M}}^{\text{o}'}$  and  $E_{\text{Agg}}^{\text{o}'}$  obtained from the Nernst plots of Figure 4, together with the monomer and aggregate optical excitation energies, an energy level diagram can be constructed that describes the thermodynamics for spectral sensitization of the cubic silver bromide microcrystals. The one-electron oxidation potential for a dye provides a measure of the energy of the HOMO and, as shown by results from photoconductivity,<sup>37</sup> ESR,<sup>38</sup> and reflectance spectroscopy<sup>39</sup> experiments, correlates with the dye's ability to trap photoholes. In Figure 9 the monomer and aggregate oxidation potentials are seen to differ by 74 mV, with the HOMO level of the monomer located at a slightly higher energy (more negative potential) than that for the aggregate. An estimate for the energetic position of the dye excited singlet state  $E^*$  can be obtained by subtracting the energy for optical excitation of the monomer and aggregate from their respective oxidation potential values.<sup>40</sup> Calculated in this manner, the oxidation potential for the singlet excited state will correlate with the ability of the photoexcited dye to inject electrons into the silver halide conduction band. Although the dye energy levels are entered as single values on the diagram of Figure 9, these positions represent the center of the redox potential distribution, which the Nernst plots suggest to be about 0.40 V in width.

Included in Figure 9 is the energetic position of the conduction band edge  $E_{\text{c}}$  for AgBr. Previous calibrations of AgBr and  $\text{AgBr}_{0.98}\text{I}_{0.02}$  using photoemission, electrochemical, and photographic data place the energy of the conduction band at about  $-1.30$  V on this aqueous electrochemical scale.<sup>41</sup>

Several important conclusions can be drawn from the energetic diagram of Figure 9. First, the fact that the monomer form of the dye is slightly easier to oxidize than the J-aggregate suggests that, in dye systems containing monomer/aggregate mixtures, the monomer may act as a shallow hole trap for the aggregate. Accordingly, if the monomer is adsorbed adjacent to or within an effective electron transfer range of the aggregate, monomer dye can supersensitize the aggregate by improving electron–hole separation, either through a mechanism involving electron transfer from the monomer to a photoexcited aggregate or from the monomer to photooxidized aggregate molecules.

This "hole-trapping" mode of sensitization efficiency improvement has been previously described as self-supersensitization and has been postulated to be operative for the J-aggregates of certain carbocyanine dyes.<sup>42</sup> Second, the energetic consequences of J-aggregation are seen to have a much larger impact on the dye excited state  $E^*$  as compared to the change reflected in the ground state (HOMO) levels. This result is consistent with theoretical calculations of the effects of packing arrangement on dye spectroscopy, which suggest that aggregation would cause a minor stabilization of the dye's ground state and a significant perturbation of the dye's excited state relative to the monomer.<sup>43</sup> For dye I the  $E^*$  of the aggregate is calculated to be ca. 0.3 V lower in energy than that of the monomer. Coincidentally, this displacement of monomer/aggregate excited state levels for dye I is seen to straddle the estimated conduction band edge for the AgBr substrate. The fortuitous location of this dye's excited-state energies with respect to the AgBr conduction band edge should lead to dramatic differences in the spectral sensitizing ability of the monomer and aggregate as discussed below.

The efficiency  $\Phi_{\text{s}}$  for dye I monomer or aggregate to spectrally sensitize AgBr is related to the rate constant  $k_{\text{inj}}$  for electron injection from the excited dye into the conduction band and to the sum of the rates  $k_{\text{q}}$  of all competing processes that quench the excited singlet state according to

$$\Phi_{\text{s}} = k_{\text{inj}} / (k_{\text{inj}} + k_{\text{q}}) \quad (5)$$

The electron injection rate depends on the overlap of the dye's donor orbital with the delocalized electronic states in the AgBr conduction band. This orbital overlap is a function of the sign and magnitude of energy gap  $[E_{\text{c}} - E^*]$  as shown in Figure 9, the reorganization energy  $\lambda$  for the electron transfer, and the spread of dye redox states due to site distribution. Given the proposal that the slope of the Nernst plot is diagnostic of the width of a Gaussian distribution of redox sites, the data above indicate that the distributions for the aggregate and monomer redox states on this cubic AgBr surface are quite similar. The reorganization energy will also contribute to the spread of dye states as  $\lambda$  reflects the distribution of states that arise from thermal fluctuations in the dielectric surrounding the dye molecule. For a given dye molecule with a site-specific ground-state oxidation potential  $E'$ ,  $k_{\text{inj}}$  is related to  $E^*$  and  $\lambda$  by the expression<sup>40b,44</sup>

$$k_{\text{inj}} \propto \exp\{-(E_{\text{c}} - E^*) + \lambda\}^2 / 4\lambda kT \} \quad (6)$$

The observed rate of electron injection will then be determined by the collection of  $k_{\text{inj}}$  terms summed over all values of  $E'$  given by the site distribution function of eq 3. The relative degree to which the dielectric fluctuations and static site-specific variations in energy contribute to the total spread of dye energies is uncertain. Estimates for the reorganization energy associated with electron injection from an excited dye into a semiconductor, including silver halide, range from 0.04 to 0.4 eV.<sup>44,45</sup> The effects of aggregation on  $\lambda$  for dye I have not specifically been determined, however, for a related dye J-aggregation was shown to lower the reorganization energy associated with electron transfer.<sup>46</sup> For the system described here, any difference in  $\lambda$  for the photoinduced redox process for the monomer and aggregate is likely to be reflected in the oxidation potential measurements of the adsorbed, ground-state dye which necessarily include a reorganizational term.<sup>4</sup> Thus, the comparative monomer/aggregate rate constants for electron injection by dye I should be largely determined by the value of  $E^*$ . If we assume that the quenching rate constants  $k_{\text{q}}$  for monomer and aggregate

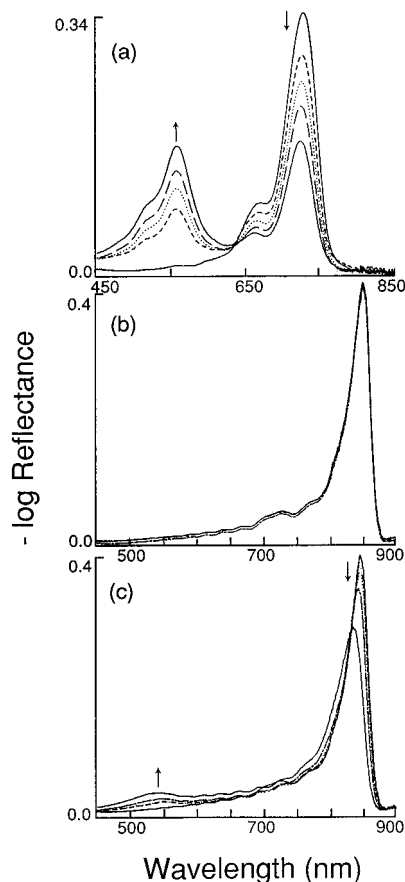


**Figure 10.** Reflectance spectra obtained before and after photoexposure of coatings of AgBr microcrystals: (a) containing adsorbed dye I monomer and exposed at 725 nm at levels ranging from 0 to 1.5 photons/molecule; (b) containing adsorbed J-aggregate and exposed at 725 nm at levels ranging from 0 to 7.8 photons/molecule; (c) containing adsorbed J-aggregate and exposed at 435 nm at levels ranging from 0 to 2.0 photons/molecule.

dye I differ only by about a factor of  $10^{47}$  then the comparative monomer/aggregate sensitization efficiencies  $\Phi_s$  will also be largely governed by energetic position of  $E^*$ , as depicted in Figure 9.

We explored the spectral sensitization of the AgBr grains containing dye I by spectrophotometrically monitoring the extent of dye bleach and radical dication formation during exposure of coatings in the region of spectral absorption by the dye. It has been shown for a variety of cyanine monomers adsorbed to cubic AgBr microcrystals that the radical dications formed as the result of a chemical oxidation are identical to the initial dye products of photosensitization.<sup>39</sup> The photosensitization experiments conducted here were of nominally "dry" coatings using the AgBr grains that were internally doped with iridium hexachloride. Previous studies have shown that iridium ions introduced into an emulsion as an internal chemical sensitizing agent are extremely effective at trapping photoelectrons in silver halide.<sup>48</sup> This characteristic of iridium sensitization was specifically used in these experiments to prevent back electron transfer, i.e., the direct recombination of the conduction band electron and the radical dication. Thus, the quantity of radical dication formed during a calibrated exposure provides a convenient measure of the efficiency for the dye to inject electrons into AgBr.

Figure 10 shows reflectance spectra obtained for coatings of monomer and aggregate dye I on AgBr as a function of light exposure using a xenon lamp filtered with narrow-band-pass interference filters. The spectra of Figure 10a were obtained

**TABLE 1: Photooxidation Results for Dye I on Ir-Doped AgBr**

aggregate state	exposure wavelength (nm)	exposure time (s)	photons absorbed $\times 10^{-14}/\text{cm}^2$ <sup>a</sup>	$f$ <sup>b</sup>	$\Phi_r$ <sup>c</sup>
M	725	0.2	0.10	0.09	0.90
M		0.5	0.24	0.17	0.71
M		1	0.43	0.29	0.67
M		2	0.70	0.48	0.69
M		5	1.52	0.58	0.38
J	850	2	1.05	0.01	0.01
J		5	2.64	0.00	0.00
J		15	7.81	0.01	0.00

<sup>a</sup> Light absorption calculated using the arithmetic mean of the film absorbance measured at dye peak before and after exposure. <sup>b</sup> Fraction of molecules oxidized. <sup>c</sup> Efficiency of radical dication production defined as radicals formed per absorbed photon.

after photoexposure at 725 nm and are nearly identical to those recorded following treatment with the ferricyanide-containing solution (radical dication  $\lambda_{\text{max}} = 553$  nm). The photoformed radical dications were very stable; no change in the reflectance spectrum of the exposed coating was observed after several hours incubation in the dark. As indicated in Table 1, the fraction  $f$  of dye converted to the radical is directly related to exposure time. At low exposure levels the photoefficiency  $\Phi_r$  for radical dication formation, and hence for electron injection  $\Phi_s$  by the excited singlet state of the adsorbed dye monomer, is very high. This result is consistent with the assigned redox levels for the monomer.<sup>49</sup> The apparent decreases in sensitization efficiency observed with the higher levels of exposure may be due in part to an inability for the iridium centers to capture all the conduction band electrons produced under these exposure conditions.

In contrast to these results for the monomer, similar exposure experiments conducted with coatings of dye I J-aggregate indicate that the aggregate *does not* impart spectral sensitivity at any of the exposure levels examined. Figure 10b shows that reflectance spectra recorded for J-aggregate coatings are unchanged following an 850 nm interference filter exposure equivalent to as much as eight photons per molecule. No evidence of dye bleach or radical dication formation was found during the spectral exposure of the dye aggregate.<sup>50</sup> These findings support our calculations that indicate the excited-state energy of the J-aggregated dye to be significantly lower in energy level than the conduction band edge of AgBr.

#### Oxidation of the J-Aggregate with Valence Band Holes.

The oxidation of dye I J-aggregate was further explored using bandgap photoexposure of the silver halide substrate. For these experiments involving a bandgap exposure where only the silver halide absorbs light, e.g., 435 nm, the conduction band electrons that are created are promptly trapped at the iridium centers, leaving reactive holes in the silver halide valence band. Cyanine radical dications can be formed via hole transfer from the silver halide valence band to the dye in its ground state.<sup>39</sup> For monomeric dye I, the spectra obtained after photoexposure at 435 nm (not shown) and at 722 nm (Figure 10) are identical and are consistent with those recorded following a chemical oxidation. For exposure levels less than one photon per molecule, the yield of radical dication photoproduct occurs with unit efficiency. Thus, virtually all of the valence band holes created during bandgap exposure arrive rapidly at the AgBr grain surface and are trapped by the adsorbed dye. This behavior is expected given that the oxidation potential of the adsorbed dye (0.355 V vs Ag/AgCl) is positioned about 1 eV above the estimated electrochemical potential of the silver bromide valence band edge (ca. 1.10 V vs Ag/AgCl).



Figure 10c illustrates that AgBr valence band holes are also energetic enough to oxidize the adsorbed dye I J-aggregate. It is noteworthy that the perturbations in the J-aggregate spectra that accompany this photooxidation process, as in Figure 10c, are of the same character as those that were induced by way of chemical oxidation (Figure 5). The spectral band associated with the J-aggregate is decreased in intensity, broadened, and blue-shifted with increased levels of 435 nm photoexposure. In addition, the appearance of the low-extinction radical dication band at ca. 535 nm is consistent with the formation of the "monomer-like" radical dication. The original spectrum of the J-aggregate can be quantitatively recovered by treatment of the photooxidized sample with dilute ascorbic acid solution. These experiments are consistent with our interpretations of the chemical oxidation of the J-aggregate as described in the previous section. In addition, the photooxidation results serve to exclude the possibility that these spectroscopic features for the oxidized aggregate are peculiar to the dye/aqueous redox mediator system.

### Conclusions

When adsorbed to the surface of cubic AgBr microcrystals, both the monomeric and J-aggregate forms of the cationic thiadycarbocyanine dye I can be reversibly oxidized with redox solutions containing ferricyanide or molybdicyanide complex. Diffuse reflectance spectra recorded for film coatings of the dyed dispersion after treatment with redox solution show distinct spectral bands associated with the dye and a stable, monooxidized dye radical ion. In the J-aggregate, the formation of the radical dications serves to partition the aggregate into smaller segments and results in a distinct shift and broadening of the aggregate reflectance band with increasing fractional degree of oxidation. That the one-electron-oxidized J-aggregate exhibits a modest degree of stability is in itself remarkable, given that the mutual electrostatic repulsive forces between the close-packed radical dications are expected to be large. These repulsive interactions may be offset by a redistribution of counter charges in the silver halide space charge layer. Overall, the observation of a stable, partially oxidized J-aggregate indicates that the electrostatic repulsion terms must be lower in magnitude than the attractive dye-dye dispersion forces and dye-AgBr adsorption forces that act to maintain the aggregate framework intact.

Nernst plots of redox solution potential  $E$  vs  $\log [\text{oxidized dye}]/[\text{dye}]$  indicate that the one-electron oxidation potential of the cyanine monomer on cubic AgBr is 74 mV less positive than that of the J-aggregate. The relative energies of the monomer and J-aggregate singlet excited states are then calculated to differ by 320 mV. These findings are consistent with the predictions of the simplified extended-dipole model that is often used to describe cyanine aggregate energetics. Because the calculated excited-state energies straddle the estimated level for the silver bromide conduction band, dramatic differences are seen in the comparative photoresponses of the monomer and aggregate dye systems. It is fortuitous that dye I exhibits favorable adsorption/aggregation properties, possesses redox levels that are in a range that are easily measured, and is optimally poised on an energetic scale for examining the effects of aggregation on spectral sensitivity. The J-aggregate is shown to be energy deficient for electron injection into AgBr, and the results from photoexposure experiments for the aggregate contrast sharply with those obtained for dye I monomer. The agreement between the photosensitivity results and the predictions of the energy level diagrams indicates that these electrochemical data provide relatively accurate measures of the energy levels meaningful to dye sensitization.

Further experiments are necessary to determine whether the magnitude and direction of these energy perturbations are characteristic of J-aggregated dye systems in a general way. The extent to which sensitization efficiency may be affected by the redox changes associated with aggregation will depend on both the particular dye and the type of semiconductor substrate. As exemplified here, these thermodynamic effects will have maximum significance when the monomer dye excited-state level and the substrate conduction band level are similar in energy. In contrast, for dyes wherein the excited-state level is positioned well above the energy of the conduction band edge, J-aggregation may have a relatively small influence on spectral sensitization efficiency.

**Acknowledgment.** We thank Dr. J. Mooberry for synthesis of the octacyanomolybdate complex and Drs. E. Brown, D. Brumbaugh, and A. Herz (retired) of Eastman Kodak Co. for many helpful suggestions.

### References and Notes

- (1) (a) Herz, A. H. *Adv. Colloid Interface Sci.* **1977**, *8*, 237. (b) Roberts, G., Ed. *Langmuir-Blodgett Films*; Plenum Press: New York, 1990.
- (2) (a) Brumbaugh, D. V.; Muentner, A. A.; Knox, W.; Mourou, G.; Wittmerhaus, B. J. *J. Lumin.* **1984**, *32*, 783. (b) Kemnitz, K.; Yoshihara, K.; Tani, T. *J. Phys. Chem.* **1990**, *94*, 3099. (c) Brumbaugh, D. V.; Muentner, A. A.; Horn, L. A.; Adams, K. A. *Excited State Dynamics in a Thiadycarbocyanine J-aggregate*; The Physics and Chemistry of Imaging Systems of the Society for Imaging Science and Technology: 1994; Vol. 1, pp 274–276.
- (3) Seefeld, K. P.; Mobius, D.; Kuhn, H. *Helv. Chim. Acta* **1977**, *60*, 2608.
- (4) Gerischer, H.; Willig, F. *Top. Curr. Chem.* **1976**, *61*, 31.
- (5) (a) Large, R. L. In *Photographic Sensitivity*; Cox, R., Ed.; Academic Press: New York, 1973; pp 241–263. (b) Tani, T.; Honda, K.; Kikuchi, S. *J. Electrochem. Soc. Jpn.* **1969**, *37*, 17. (c) Lenhard, J. R. *J. Imaging Sci.* **1986**, *30*, 27.
- (6) (a) Gilman, P. B. *Pure Appl. Chem.* **1977**, *49*, 357. (b) Leubner, I. *Photogr. Sci. Eng.* **1976**, *20*, 61. (c) Leubner, I. *Photogr. Sci. Eng.* **1978**, *22*, 270. (d) Tani, T. *J. Imaging Sci.* **1988**, *33*, 17. (e) Lenhard, J. R.; Hein, B. R.; Muentner, A. A. *J. Phys. Chem.* **1993**, *97*, 8269.
- (7) Sturmer, D. P. In *Kirk-Othmer Encyclopedia of Chemical Technology*, 3rd ed.; Interscience: New York, 1979; p 393.
- (8) Herz, A. H. *Photogr. Sci. Eng.* **1974**, *18*, 323.
- (9) (a) Makio, S.; Kanamaru, N.; Tanaka, J. *Bull. Chem. Soc. Jpn.* **1980**, *53*, 3120. (b) Matsubara, T.; Tanaka, T. *J. Imaging Sci.* **1991**, *35*, 274.
- (10) Furman, N. H.; Miller, C. O. *Inorg. Synth.* **1950**, *3*, 160.
- (11) (a) Berry, C. R.; Skillman, D. C. *Photogr. Sci. Eng.* **1962**, *6*, 159. (b) Gilman, P. B. *J. Photogr. Sci.* **1983**, *31*, 185.
- (12) (a) The equilibrium constant for adsorption of TSSA to AgBr is slightly less than that measured for adsorption of a cationic sensitizing dye. (b) When adsorbed to cubic AgBr at 35 °C in the absence of TSSA, mixtures of dye I monomer and J-aggregate can be obtained.
- (13) As discussed in ref 1a, the magnitude of this spectral shift is a function of the dielectric constant of the silver halide and of the dye  $\lambda_{\text{max}}$ .
- (14) The spectrum of Figure 1B also indicates that, under the conditions for adsorption of dye I as the aggregate, a trace amount of dye is adsorbed in the monomeric state.
- (15) The spectrum of dye I radical dication is typical of that found for oxidized cyanines as reported in: Lenhard, J. R.; Cameron, A. D. *J. Phys. Chem.* **1993**, *97*, 4916.
- (16) For the adsorbed dye I monomer, the relative intensities of the reflectance bands at 722 and 553 nm indicate the adsorbed radical dication to have an apparent extinction coefficient that is 0.67 times that of the dye. In methanol solution the ratio of extinction coefficients is 0.62.
- (17) (a) Laviron, E. *J. Electroanal. Chem. Interfacial Electrochem.* **1974**, *52*, 395. (b) Brown, A. P.; Anson, F. C. *Anal. Chem.* **1977**, *49*, 1589. (c) Laviron, E. *J. Electroanal. Chem. Interfacial Electrochem.* **1975**, *63*, 245.
- (18) (a) Albery, W. J.; Boutelle, M. G.; Colby, P. J.; Hillman, A. R. *J. Electroanal. Chem.* **1982**, *133*, 135. (b) Chidsey, C. E. D.; Bertozzi, C. R.; Putvinski, T. M.; Mujcs, A. M. *J. Am. Chem. Soc.* **1990**, *112*, 4301. (c) Jiang, R.; Anson, F. C. *Electroanal. Chem.* **1991**, *305*, 171. (d) Sabatani, E.; Anson, F. C. *J. Phys. Chem.* **1993**, *97*, 10158. (e) Rowe, G. K.; Carter, M. T.; Richardson, J. N.; Murray, R. W. *Langmuir* **1995**, *11*, 1797.
- (19) (a) Nechtschein, M.; Devreux, F.; Genoud, F.; Vieil, E.; Pernaut, J. M.; Genies, E. *Synth. Met.* **1986**, *15*, 59. (b) Ameniya, T.; Hashimoto, K.; Fujishima, A. *J. Electrochem. Soc.* **1991**, *138*, 2845.
- (20) Gerischer, H.; Scherson, D. A. *J. Electroanal. Chem. Interfacial Electrochem.* **1982**, *133*, 135.

- (21) (a) Bowden, E. F.; Dautartas, M. F.; Evans, J. F. *J. Electroanal. Chem.* **1987**, 219, 91. (b) Braun, H.; Storck, W.; Doblhofer, K. *J. Electroanal. Chem.* **1980**, 115, 143.
- (22) (a) Bowden, E. F.; Dautartas, M. F.; Evans, J. F. *J. Electroanal. Chem.* **1987**, 219, 49. (b) Dautartas, M. F.; Bowden, E. F.; Evans, J. F. *J. Electroanal. Chem.* **1987**, 219, 71. (c) Marque, P.; Roncali, J. *J. Phys. Chem.* **1990**, 94, 8614.
- (23) Smith, C. P.; White, H. S. *Anal. Chem.* **1992**, 64, 2398.
- (24) At pH 2.1, the gelatin glycine sites are partially protonated, and the gelatin acquires polyelectrolyte properties.
- (25) Steiger, R.; Aebischer, J.-N.; Haselbach, E. *J. Imaging Sci.* **1991**, 35, 1.
- (26) (a) Chen, S. Y.; Horng, M. L.; Quitevis, E. L. *J. Phys. Chem.* **1989**, 93, 3683. (b) Quitevis, E. L.; Horng, M. L.; Chen, S. Y. *J. Phys. Chem.* **1988**, 92, 256. (c) Kemnitz, K.; Yoshihara, K.; Tani, T. *J. Phys. Chem.* **1990**, 94, 3099.
- (27) (a) West, W. *Nature* **1961**, 191, 902. (b) Sturmer, D. M.; Gaugh, W. S.; Bruschi, B. J. *Photogr. Sci. Eng.* **1974**, 18, 49. (c) Yianoulis, P.; Nelson, R. C. *Photogr. Sci. Eng.* **1974**, 18, 94. (d) Gunther, E.; Moisar, E. *J. Photogr. Sci.* **1965**, 13, 280. (e) Gilman, P. B.; Penner, T. L. *Photogr. Sci. Eng.* **1984**, 28, 238.
- (28) The dye concentration range examined was limited at low coverage by instrument sensitivity and at high coverage by the onset of J-aggregation.
- (29) In acetonitrile, the removal of a second electron from monomeric dye I can be accomplished electrochemically at a potential of ca. 1.2 V. This second oxidation is irreversible, and the trication formed is very unstable. This higher oxidation state for dye I is not achievable with the ferricyanide or molybdcyanide redox buffers.
- (30) An unambiguous determination of the effect of adsorption on dye potential requires knowledge of the oxidation potential for dye I dissolved in the aqueous phosphate buffer. Dye I is not soluble in this buffer solution.
- (31) Chemical oxidation of methanol/water solutions of cyanine H- or J-aggregates yields oxidized cyanine molecules in the unassociated state.
- (32) The formal oxidation potentials, determined at a glassy carbon electrode, for the hexacyanoferrate and octacyanomolybdate redox couples in this buffer system are 0.28 and 0.57 V vs Ag/AgCl, respectively.
- (33) (a) Muentner, A. A.; Brumbaugh, D. V.; Apolito, J.; Horn, L. A.; Spano, F. C.; Mukamel, S. *J. Phys. Chem.* **1992**, 96, 2783. (c) Spano, F. C.; Mukamel, S.; Kuklinski, J. R.; Brumbaugh, D. V.; Burberry, M. S.; Muentner, A. A. *Mol. Cryst. Liq. Cryst.* **1991**, 194, 331.
- (34) According to the point-dipole approximation the transition energy will vary as a function the size of the aggregate according to  $S_n = S_M - [(n-1)/n][S_M - S_\infty]$ , where  $S_n$  is the transition energy of an aggregate of length  $n$ , and  $S_M$  and  $S_\infty$  are the transition energies for the monomer and infinite aggregate, respectively. See: McRae, E. G.; Kasha, M. *J. Chem. Phys.* **1958**, 28, 721.
- (35) The similarity in the spectral bandwidth changes for the aggregate dilution and aggregate oxidation also supports a model wherein the oxidized molecules are distributed as shown in Figure 8. An alternate model where the oxidized sites are located at the edges of the aggregate would give a different distribution of aggregate sizes and different spectral bandwidth changes.
- (36) Knowing the total number of dye molecules per AgBr grain, the oxidized dye/unoxidized dye ratio for the aggregate was calculated from the magnitude of the 842 nm band. However, the J-aggregate dilution data of Figure 7 indicate that when the fractional degree of oxidation exceeds 60%, the proportionality between concentration and  $[1/R]$  is compromised because of broadening of the aggregate band. The Nernst plot for the aggregate included only those points derived within the linear region.
- (37) Saunders, V. I. *Photogr. Sci. Eng.* **1977**, 21, 163.
- (38) Tani, T. *J. Appl. Phys.* **1987**, 62, 2456.
- (39) Lenhard, J. R.; Muentner, A. A. In *Photoelectrochemistry and Electrosynthesis on Semiconducting Materials*; Ginley, D. S., Ed.; The Electrochemical Society: Pennington, NJ, 1988; Proc. Vol. 88-14, pp 97-104.
- (40) (a) Rehm, D.; Weller, A. *Ber. Bunsen-Ges. Phys. Chem.* **1969**, 73, 834. (b) Gerischer, H. *Photochem. Photobiol.* **1972**, 16, 243.
- (41) As discussed in ref 6e,  $E_c$  is equivalent to a monomeric dye having a reduction potential in acetonitrile of  $-0.92$  V vs Ag/AgCl.
- (42) (a) Simpson, J. M. *Photogr. Sci. Eng.* **1974**, 18, 302. (b) West, W.; Gilman, P. B. Jr. *Photogr. Sci. Eng.* **1969**, 13, 221. (c) Gilman, P. B., Jr. *Photogr. Sci. Eng.* **1974**, 18, 418.
- (43) Hochstrasser, R. M.; Kasha, M. *Photochem. Photobiol.* **1964**, 3, 317.
- (44) Spitler, M. *J. Imaging Sci.* **1991**, 35, 351.
- (45) (a) Trosken, B.; Willig, F.; Schwarzburg, K.; Ehret, A.; Spitler, M. *J. Phys. Chem.* **1995**, 99, 5152. (b) Kietzmann, R.; Ehret, A.; Spitler, M.; Willig, F. *J. Am. Chem. Soc.* **1993**, 115, 1930. (c) Tani, T.; Suzumoto, T.; Ohzeki, K. *J. Phys. Chem.* **1990**, 94, 1298.
- (46) As reported in ref 45a,  $\lambda$  for a J-aggregated anionic dye was found to differ from that of a cationic monomeric dye by a factor of 10. We expect a much smaller difference in  $\lambda$  for a monomer/aggregate pair derived from the same chromophore with the same net charge.
- (47) Even a 100-fold difference in  $k_q$  between dye I monomer and aggregate cannot account for the drastic difference in  $\Phi_s$  of Table 1. As shown in ref 2c for a thiacyanocyanine monomer and J-aggregate adsorbed to AgBr, a 100-fold difference  $k_q$  results in only a 40% difference in spectral sensitization efficiency.
- (48) Berriman, R. W.; Gilman, P. B. *Photogr. Sci. Eng.* **1973**, 17, 235.
- (49) Relative quantum efficiencies of spectral sensitization were also measured using standard photographic techniques on coatings prepared using a companion AgBr dispersion containing no iridium dopant. These measurements indicate a quantum efficiency  $>0.9$  for the monomer, whereas the J-aggregate afforded no spectral sensitivity to the silver halide.
- (50) (a) In a similar exposure experiment using a related thiacyanocyanine adsorbed as a monomer with an absorption maximum at 850 nm and an estimated  $E^* \approx E_c$ , a  $\Phi_r$  of 0.8 was obtained, showing that spectral sensitization of AgBr at this wavelength is feasible for a dye with the appropriate redox levels.